Acupuncture and Herbal Medicine

OPEN

Water extracts of *Polygonum Multiflorum* Thunb. and its active component emodin relieves osteoarthritis by regulating cholesterol metabolism and suppressing chondrocyte inflammation

Lanqing Li[1], Haiying Xu[1], Linghang Qu[1], Maryam Nisar[2], Muhammad Farrukh Nisar[2], Xianqiong Liu[1,*], Kang Xu[1,*]

Abstract

Objective: *Polygonum multiflorum* Thunb. (PMT) is a widely used traditional Chinese herbal medicine with a variety of pharmacological effects. This study investigates the chemical composition of a water extract of PMT and its potential as a therapy for osteoarthritis (OA).

Methods: The components of the aqueous extract of PMT were determined using high-performance liquid chromatography (HPLC). Gene ontology and Kyoto Encyclopedia of Genes and Genomes pathway enrichment analyses of a gene expression dataset downloaded from the Gene Expression Omnibus (GEO) were performed using Limma in R language. Differential chondrocyte metabolites were determined using gas chromatography-mass spectrometry (GC-MS) before and after treatment.

Results: The water extract of PMT showed good ability in improving OA, and the content of the active ingredient emodin increased significantly after processing. Analysis of the GEO database further demonstrated a strong association between OA and metabolic pathways. Emodin promotes chondrocyte proliferation and significantly reduces the number of inflammatory factors. The metabolomic results showed that emodin affected five metabolic pathways related mainly to primary bile acid biosynthesis, steroid biosynthesis, and biosynthesis of unsaturated fatty acids.

Conclusions: This study revealed the pharmacological effects of PMT and emodin as the main active components, thereby providing a scientific basis for the treatment of OA.

Keywords: Blood components, Emodin, Metabonomics, Osteoarthritis, *Polygonum multiflorum* Thunb.

Graphical abstract: http://links.lww.com/AHM/A51.

Introduction

Osteoarthritis (OA) is a common chronic joint disease that can lead to the loss of motion and function. It is mainly characterized by progressive destruction of articular cartilage and osteophytes, frequently accompanied by joint inflammation and pain[1]. Age, obesity, and genetics are important factors that contribute to the development of OA[2–3]. Approximately 240 million people worldwide suffer from OA[4–5]. Various surgical and nonsurgical treatment options are available[6]. Surgical treatment mainly involves arthroplasty and joint fusion, whereas non-operative treatments include oral or intra-articular injection of non-steroidal anti-inflammatory drugs (NSAIDs) or glucocorticoids and general treatments such as physiotherapy or varus thrust[7–8]. However, existing treatment modalities have major limitations and side-effects. Surgical treatments are limited by age or physical fitness and are therefore not applicable to all patients with OA. In addition, the long-term use of NSAIDs as first-line drugs for OA can lead to gastrointestinal irritation, ulceration, and bleeding[9]. Therefore, new therapeutic strategies and drugs that overcome these limitations with minimal side-effects are urgently required.

Disturbances in the metabolic environment are important triggers for OA development. Lipid metabolism disorders can lead to the accumulation of lipids that can destroy cartilage and reduce bone densitometry and mass[10]. Glucose metabolism disorders can upregulate inflammatory factor levels through oxidative stress and increased inflammation, causing cartilage degradation and further aggravating OA[11]. Disorders of bone

Lanqing Li and Haiying Xu contributed equally to this study.

[1]Hubei Engineering Technology Research Center of Chinese Materia Medica Processing, College of Pharmacy, Hubei University of Chinese Medicine, Wuhan 430065, China; [2]Department of Physiology and Biochemistry, Cholistan University of Veterinary and Animal Sciences (CUVAS), Bahawalpur, 63100, Pakistan

**Corresponding author: Kang Xu, Hubei Engineering Technology Research Center of Chinese Materia Medica Processing, College of Pharmacy, Hubei University of Chinese Medicine, Wuhan 430065, China, E-mail: kangxu05@hbtcm.edu.cn; Xianqiong Liu, Hubei Engineering Technology Research Center of Chinese Materia Medica Processing, College of Pharmacy, Hubei University of Chinese Medicine, Wuhan 430065, China, E-mail: 1424@hbtcm.edu.cn.*

Acupuncture and Herbal Medicine (2023) 3:2

Received 22 November 2022 / Accepted 20 February 2023

http://dx.doi.org/10.1097/HM9.0000000000000061

metabolism can lead to joint inflammation mainly through the degradation of cartilage and osteophytes[12]. Many other metabolic pathway disorders exacerbate the development of OA. Therefore, targeting metabolic pathways may be beneficial in the treatment of human OA.

Traditional Chinese medicine (TCM) has shown good therapeutic effects with few side-effects in clinical practice. *Polygonum multiflorum* Thunb. (PMT) is a popular Chinese herbal medicine (CHM) with many pharmacological effects including anti-inflammatory and anti-oxidation properties[13–14]. PMT is one of the main ingredients of *Shouwu Yanshou Dan* (SWYSD), which has been shown to prevent and treat OA[15]. According to the TCM theory, appropriate processing can reduce toxicity and improve the curative efficacy of CHMs[16]. The free anthraquinone content of PMT increased after processing, and emodin was identified as the main component. Though emodin has showed good anti-inflammatory effects[17–18], its potential to treat OA by modulating metabolism has not been reported.

In this study, we used metabolomics techniques to investigate the ability of processed PMT to improve OA by regulating metabolic pathways.

Materials and Methods

Preparation of rat chondrocyte cultures

Cartilage tissues were obtained from the knee joints of healthy male Sprague–Dawley rats (n = 5, body weight: 50 g). The cartilage tissue was cut into small pieces, gently rinsed with phosphate-buffered saline (PBS) (Aspen, Wuhan) and 1% penicillin-streptomycin (Solarbio, Beijing) and transferred to culture flasks containing 2 mg/mL collagenase type II (Sigma, Santa Clara, California). After incubation for 2 to 4 h at 37°C under 5% CO_2, the medium was replaced with DMEM/F12 (1:1, Gibco, Grand island, New York) containing 10% FBS (Gibco, Grand island, New York). Second and third-passage chondrocytes were used in the experiments. All animal experiments were approved by the Institutional Review Board of Hubei University of Chinese Medicine.

Emodin and TNF-α treatment

Stock solutions (100 mM) of emodin (Shanghai Yuanye Biotechnology, Ltd., Shanghai, China) and dexamethasone (DEX; Selleck Chemicals, USA) were prepared separately by dissolving them in dimethyl sulfoxide (DMSO). Rat chondrocytes were treated with different concentrations (5, 10, 20, 40, and 80 μM) of emodin, and DMSO was used as a control. Morphological changes in cells were observed under a microscope. In addition, chondrocytes were treated with 10 ng/mL tumor necrosis factor (TNF) -α alone (TNF-α–treated group), TNF-α + emodin 20 μM (TNF-α + emodin-treated group), or TNF-α + DEX 10 μM (TNF-α + DEX-treated group) for 24 h (with TNF-α and emodin or TNF-α and DEX added in the same order). All experiments were performed independently and in triplicates.

Cell viability assay

Cell viability and drug toxicity were evaluated using the Cell Counting Kits 8 (CCK-8, Beyotime, Beijing, China). Rat primary chondrocytes were seeded in 96-well plates (5,000 cells/well) and treated with different concentrations of emodin, DMSO was used as the control. After 24 h, the cells were incubated with the CCK-8 reagent for 2 to 4 h at 37°C. The absorbance in each well was measured at 450 nm using a microplate reader (BioTek, Santiago, California). All experiments were performed independently and in triplicates.

RT-qPCR and data analysis

Rat chondrocytes were seeded in 6-well plates and treated for 24 h with TNF-α or TNF-α + emodin, DMSO was used as a control. TRIzol (1 mL) reagent (Invitrogen, Thermo Scientific, USA) was added to each well and total RNA was extracted by scratching the cells at each corner of the bottom of the six-well plate with a 1,000 μL gun. After purification, RNA was used as a template to generate cDNA by reverse transcription using a commercial kit (ABclonal Co., Ltd., RK20429). cDNA was used as a template for the RT-qPCR analysis of gene expression. The NCBI website was used to design primers, and the accuracy of the primers was verified using BLAST. Finally, Invitrogen was used for synthesis. The primer sequences used are listed in Supplementary Table 1, http://links.lww.com/AHM/A50. The data were analyzed using the $2^{-\Delta\Delta ct}$ method (Table 1).

Western blotting analysis

Rat chondrocytes were seeded in six-well plates and treated for 24 h with TNF-α or TNF-α + emodin, DMSO

Table 1.

Sequences of the real-time qPCR

	RT-qPCR primers	
Gene name	**Forward**	**Reverse**
ACAN	AACTTCTTCGGAGTGGGTGGT	CAGGCTCTGAGACAGTGGGG
COL2A	AATTTGGTGTGGACATAGGG	AAGTATTTGGGTCCTTTGGG
IL-6	CCTGAACCTTCCAAAGATGGC	TTCACCAGGCAAGTCTCCTCA
IL-1β	TGACTTCACCATGGAACCCG	GACCTGACTTGGCAGAGGAC
PTGS2	ATTACTGCTGAAGCCCACCC	GGCCCTGGTGTAGTAGGAGA
MMP1	TAGGTGTGGGGTGCCTGATG	GCTCTCTCGATGGCGTTTTCT
MMP3	AATCCCTCTATGGACCTCCCAC	AAGAACAAGACTTCTCCCCGC
MMP13	ACCCAGCCCTATCCCTTGAT	TCTCGGGATGGATGCTCGTA
β-actin	TCCCTGGAGAAGAGCTATGA	ATAGAGCCACCAATCCACAC

was used as a control. Lysis was performed using RIPA protein extraction reagent (Beyotime). After SDS-polyacrylamide gel electrophoresis, the proteins were transferred onto PVDF membranes, which were then closed with 5 % skim milk powder for 1 h, and the membranes were incubated with the antibodies overnight at 4°C. It was then washed thrice with TBST for 5 min each and incubated with a secondary antibody (rabbit or mouse antibody) for 1 h at 25°C. Finally, the PVDF membrane was washed thrice with TBST for 5 min each. A chemiluminescent reagent (WBKLS0010, Millipore) was added for the immunoassay. The protein bands were observed using a Tanon-4800 system (Tanon, Beijing, China). The gray scale values of each band were analyzed using Tanon software and quantified using Image-J (V1.8.0).

Preparation of samples for GC-MS analysis

Rat chondrocytes were seeded in six-well plates and treated for 24 h with TNF-α or TNF-α + emodin, DMSO was used as a control. The cell surface was then quickly and gently rinsed twice with 37°C in 0.9% saline. Next the cells were rinsed twice with pre-cooled PBS. The six-well plate was transferred to ice, and 250 μL of −80°C pre-cooled methanol solution was added. They were then placed in liquid nitrogen for 10 min and thawed at room temperature for 5 min, followed by repeated freezing and thawing thrice. The freeze-thawed samples were centrifuged at 4°C at 12,000 rpm. The supernatant was transferred to a new EP tube and dried at 37°C using a nitrogen blower. The samples were then processed using a two-step method. First, 80 μL of methoxypyridine solution (20 mg/mL) was added, centrifuged for 2 min and incubated for 2 h at 37°C. Then 80 μL BSTFA was added, centrifuged for 2 min, and incubated for 1 h in a water bath at 80°C. Finally, the processed samples were transferred into 200 μL sample tubes and metabolomic analysis was performed using a Trace 1300 GC-MS System (Thermo, USA).

GC-MS analysis

The system was equipped with a DB-5MS capillary column (30 m × 250 μm inner diameter, 0.25 μm film thickness). High-purity helium was used as the carrier gas at a flow rate of 1.0 mL/min. The feeder split ratio was set at 10:1. The temperatures of the mass spectrometer, ion source, and injector were 280°C, 200°C, and 280°C, respectively. The sample volume for injection was 1 μL at a time. A full scan was conducted with an initial temperature of 80°C and a mass-to-charge ratio (*m*/*z*) between 50 and 650 Da[19–21].

Drug preparation

Black beans were purchased from Nantong, Jiangsu, China, and PMT tablets were purchased from Beijing Huamiao Pharmaceutical Company Ltd. (Beijing, China; XE3141). An appropriate amount of PMT tablet was added to 10 times the volume of water and boiled for 2 h. Water was collected before eight times the volume of water was added, and the tablets were boiled for the second time for 1.5 h. The two decoctions were combined and concentrated to obtain PMT aqueous extract (group S). Treated black beans were added to water (eight volumes) and boiled for approximately 4 h, before adding a further eight volumes of water to the soybean dregs and boiling for approximately 3 h. The two decoctions were combined and concentrated to obtain the final black bean to black-bean-juice ratio of 1:2.5. Appropriate amounts of raw PMT slices were immersed in black bean juice at a black bean/PMT ratio of 1:10. When all black bean juice was absorbed, the mixture was placed in an appropriate container and steamed until the PMT turned brown. Finally, the water extract of the PMT-processed product (group Z) was prepared using PMT water extract treatment method.

High-performance liquid chromatography analysis

The chromatographic column was an Agilent Extend C_{18} column (250 mm × 4.6 mm, 5 μm). Mobile phases A (acetonitrile) and B (0.1% phosphate) were used, and all mobile phases were chromatographically pure. For the injection analysis, the sample volume was 10 μL, and the flow rate was 1 mL/min. Linear gradient elution was performed as follows: 0 to 10 min, 10% to 20% A; 10 to 15 min, 20% to 30% A, 15 to 30 min, 30% to 45% A, 30 to 35 min, 45% to 80% A, 35 to 40 min, 80% to 90% A, 40 to 60 min, 90% to 10% A.

Animal model of OA

Sprague–Dawley rats weighing 200 to 250 g were purchased from the Hubei Research Center of Laboratory Animals (license number: SCXK (Hubei, China) 2020-0018; Certificate No.: 42000600048137). The OA model was established in 70 Sprague–Dawley rats (200–250 g) according to a previous report[22]. OA was induced by a single injection of sodium iodoacetate (6 mg/kg body weight, 50 μL) into the knee joint. The rats were maintained at 25°C to 27°C, with free access to food and water. OA rats were then randomly divided into seven groups: control, sodium iodoacetate model group (MIA), diclofenac sodium enteric-coated tablet suspension group (DIC, 6 mg/kg), S low-dose group (SD 600 mg/kg), S high-dose group (SG 1,200 mg/kg), Z low-dose group (ZD 1,200 mg/kg), and Z high-dose group (ZG 2,400 mg/kg). After 4 weeks of drug treatment, the rats were euthanized by pentobarbital sodium anesthesia followed by cervical dislocation. Knee joint specimens were collected for macroscopic and microscopic examinations. This animal study was reviewed and approved by the Animal Care Committee of the Hubei University of Chinese Medicine (approval: No. 00273285, November 10, 2021).

Histological analysis

After 31 d of MIA treatment, knee samples were collected from OA model animals and fixed in 4% paraformaldehyde for 2 d. Subsequently, the samples were decalcified in 10% EDTA solution for 1 month, and the EDTA solution was changed every 3 d. Finally, the samples were dehydrated in a series of alcohol solutions and placed in 75% ethanol for long-term storage. Dehydrated knee samples

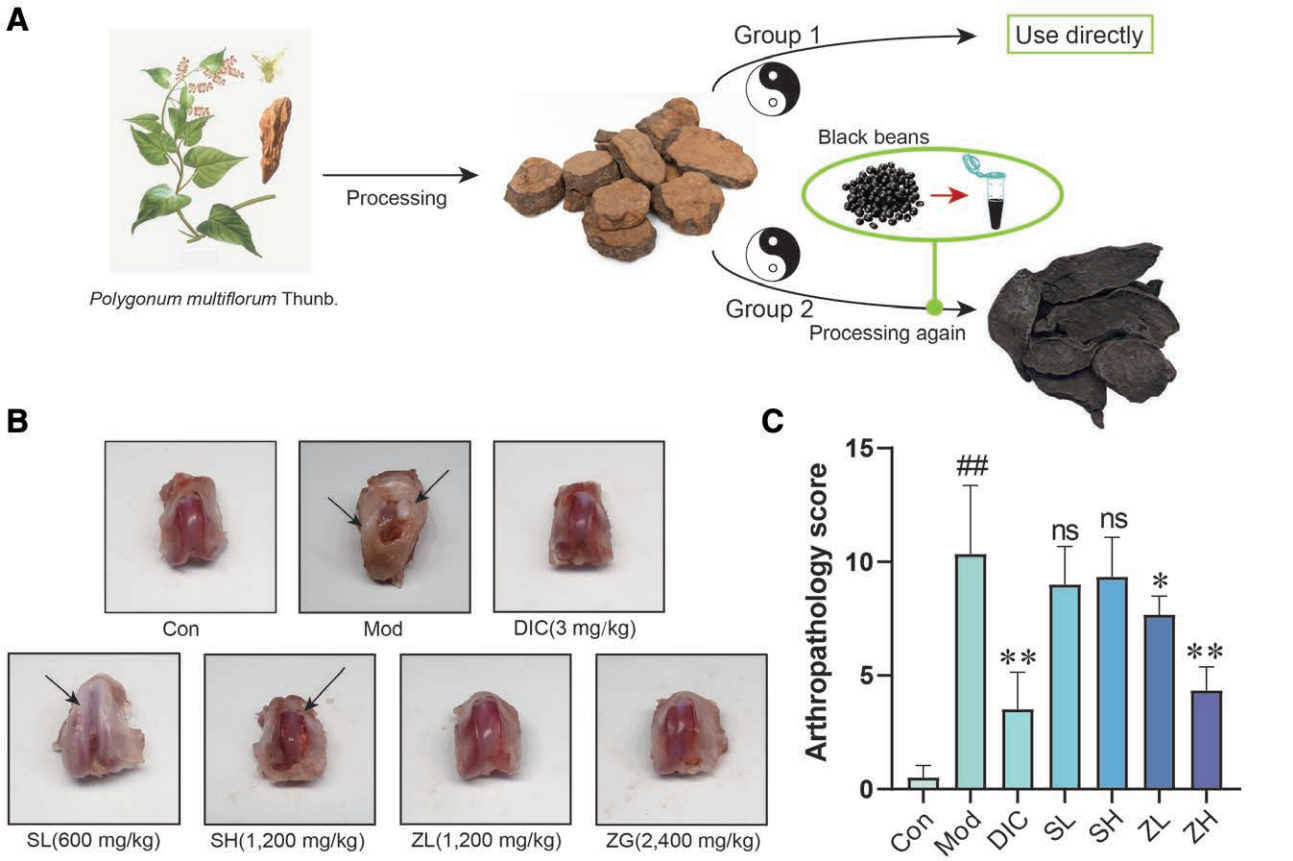

Figure 1. Macroscopic evaluation of knee cartilage after PMT treatment. (A) Flow chart of PMT water extract preparation. (B) Necrosis is indicated by a black arrow. (C) Pathology scores. $^{\#\#}P < 0.01$ versus the control Con group; $^{*}P < 0.05$, $^{**}P < 0.01$ versus the Mod group. PMT: *Polygonum multiflorum* Thunb.

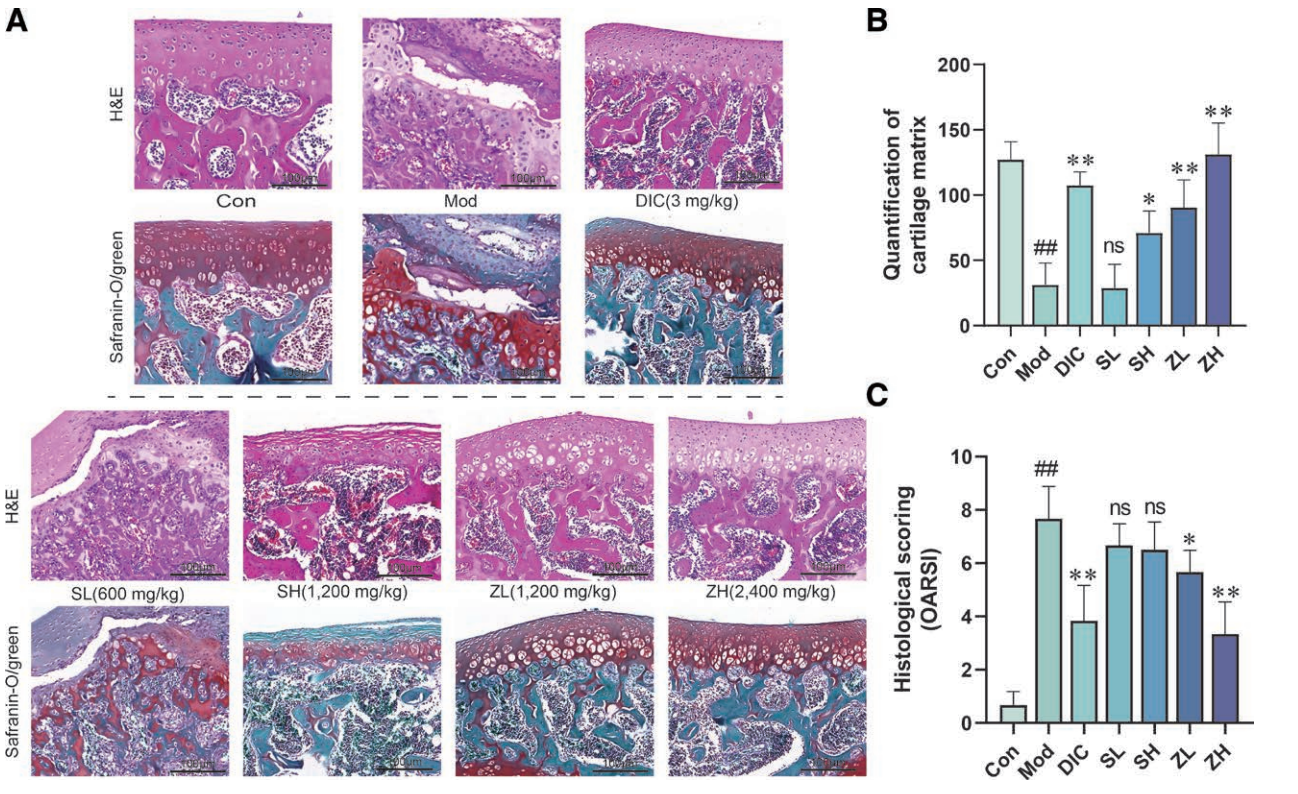

Figure 2. Histological analysis of knee cartilage after PMT treatment. (A) H&E and Safranin-O/green staining after 31 d of MIA administration. (B) Quantitative analysis of the Safranin-O/green staining. (C) OARSI score. $^{\#\#}P < 0.01$ versus the control Con group; $^{*}P < 0.05$, $^{**}P < 0.01$ versus the Mod group. PMT: *Polygonum multiflorum* Thunb.; MIA: Monosodium Iodoacetate; OARSI: Osteoarthritis Research Society International.

were embedded in paraffin and sectioned to a thickness of 10 μM. All samples were stained with hematoxylin and eosin (H&E) and Safranin-O/green. H&E staining was performed to observe changes in the surface of the articular cartilage, cartilage levels, and number and morphology of cartilage cells.

Statistical analysis

One-way analysis of variance (ANOVA) was performed on the data using SPSS 22.0 and GraphPad Prism 8.0. Significant differences between groups were determined and expressed as the mean ± standard deviation (SD), $P < 0.05$ was considered statistically significant.

Results

PMT-processed water extract alleviates cartilage degeneration induced by sodium iodoacetate (MIA) in rats

The PMT water extract was divided into two groups, with high- and low-dose groups for each defined as the PMT water extract groups (SL, SH) and the processed water extract groups (ZL, ZH) (Figure 1A). An OA model was established by intra-articular injection of MIA, and healthy rats were used as the control group. Visual observation of the rat knee joint showed significant cartilage degeneration in the Mod group and minimal visible lesions in the remaining treatment groups (Figure 1B). The histological scores of each group were significantly different from those of the Mod group (Figure 1C, $P < 0.01$)[23], with higher scores representing greater cartilage damage ($P < 0.05$ or $P < 0.01$).

H&E and safranin-O/green staining revealed the normal morphology of the cartilage cells in the Con group. The cartilage matrix was rich, and the tide line was complete. In contrast, the Mod group exhibited varying degrees of cartilage degradation. Similar to the Mod group, thinning of the cartilage matrix and degradation of the cartilage were observed in the SL and SH groups. The cartilage in the positive drug group [Diclofenac Sodium Enteric-coated Tablets (DIC)] and the ZL and ZH groups were more similar to that of the Con group,

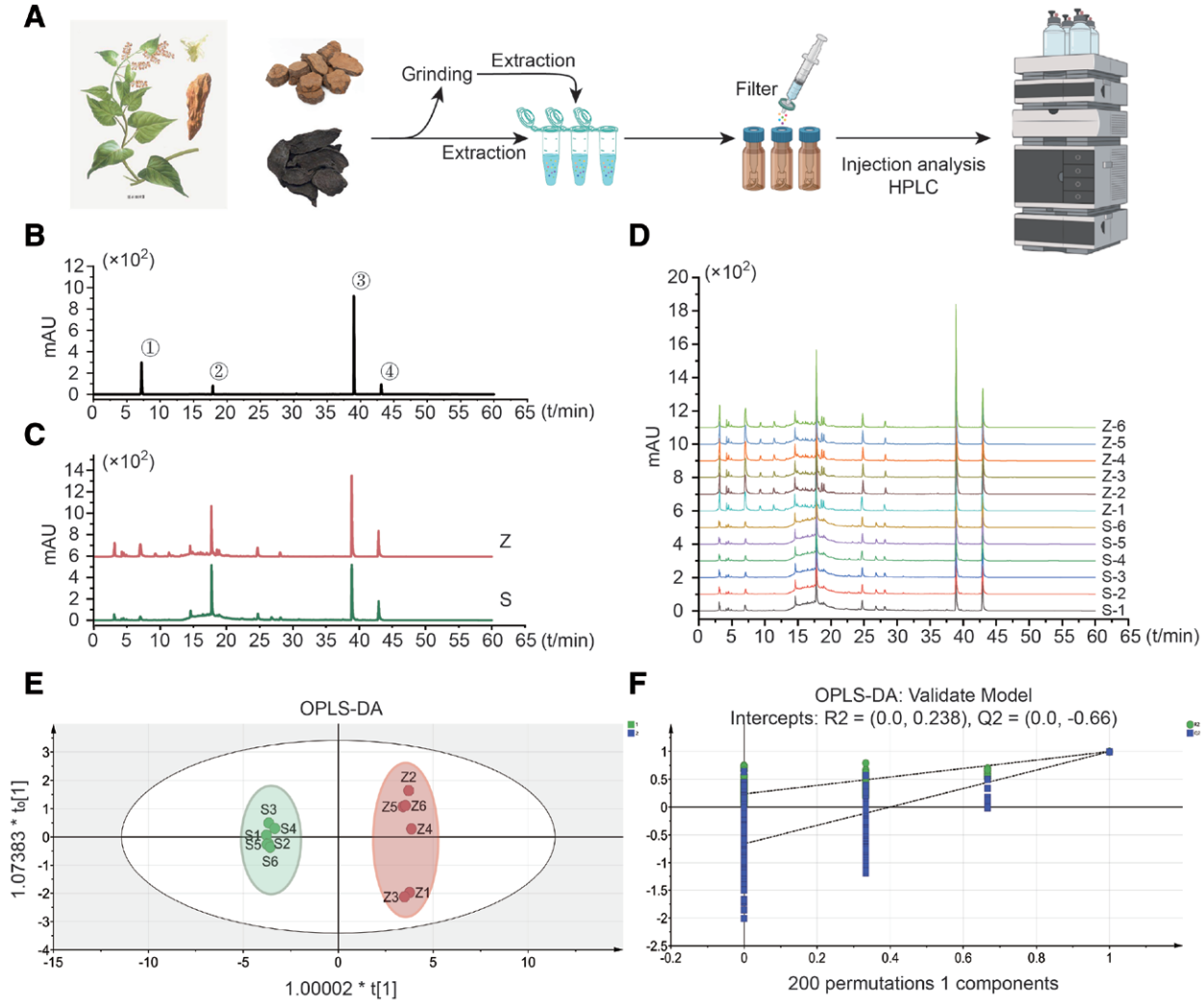

Figure 3. HPLC chromatograms of water extracts of PMT decoction pieces S and Z groups. (A) HPLC sample preparation flow chart of PMT prepared slices S and Z groups. (B) Mixed control chart. ①. Gallic acid; ②. stilbene; ③. Emodin; ④. Physcion. (C) Water extract atlas of PMT prepared slices in groups S and Z. (D) Characteristic atlas of water extracts from six batches of PMT prepared slices in groups S and Z. (E) OPLS-DA diagram of water extracts of six batches of PMT prepared slices in groups S and Z. (F) Two hundred permutations of the OPLS-DA model for serum. HPLC: High-performance liquid chromatography; PMT: *Polygonum multiflorum Thunb.*; OPLS-DA:Orthogonal Partial Least Squares Discriminat.

with an intact tide line and no osteophytes (Figure 2A). In addition, there were significant differences in the OARSI scores and quantitative analysis of safranin-O/green staining between the Mod and Con groups ($P < 0.05$). The treatment effect was more pronounced in the DIC group than in the ZL and ZH groups (Figure 2B, C, $P < 0.05$). These results show that ZL and ZH inhibited cartilage matrix degradation and promoted cartilage matrix recovery, which may contribute to improvements in OA symptoms.

Analysis of the chemical composition of the water extract of PMT before and after processing

High-performance liquid chromatography (HPLC) analysis of the PMT water extracts before and after processing was performed (Figure 3A). The mixed reference substances, gallic acid, stilbene, emodin, and physcion (Figure 3B), were used to identify the main active components of the PMT water extract samples according to the corresponding retention times (Figure 3C). Emodin was identified as the major component, and the content of the water extract of emodin significantly increased after concoction. To ensure the stability of the preparation process, we prepared six batches of S and Z simultaneously (Figure 3D). The OPLS-DA analysis model we developed showed that the S and Z groups clustered into one category separately, and the S and Z groups were well differentiated (Figure 3E). The 200 external validations demonstrated the good predictive power of the OPLS-DA model (Figure 3F).

Cytotoxic effects of emodin on chondrocytes

The chemical structure of emodin has been presented in Figure 4A. The CCK-8 assay was used to investigate the cytotoxic effects of emodin on rat chondrocytes. Emodin (10 μM) promoted chondrocyte activity, while the viability was significantly decreased by emodin ≥ 20 μM (Figure 4B). The IC50 value of emodin for chondrocytes was 28.57 μM (Figure 4C). Therefore, 10 μM emodin was used in this study. Chondrocyte proliferation was evaluated after 5 days of emodin treatment. Compared with the DMSO group, 10 μM emodin treatment promoted chondrocyte proliferation (Figure 4D), whereas emodin treatment at 5 to 10 μM had no significant effect on chondrocytes. After treatment with emodin at ≥40 μM, a significant decrease in the number of chondrocytes and significant morphological changes were observed (Figure 4E).

Emodin improves TNF-α-induced gene and protein expression in vitro

TNF-α treatment of chondrocytes leads to decreased expression of ACAN and COL2A, and increased expression of inflammatory factors. Degradation of the chondrocyte matrix and increased inflammation further contribute to the development of OA. To explore the protective effects of emodin on TNF-α–treated chondrocytes, we examined the expression of related genes and proteins using RT-qPCR and Western blotting. TNF-α treatment decreased the mRNA expression of ACAN and COL2A, while emodin (10 μM) and DEX treatment restored the mRNA expression of ACAN and COL2A. As shown in Figure 5A, TNF-α treatment increased the mRNA expression levels of IL-1β, IL-6, MMP1, MMP3, MMP13, and PTGS2, whereas emodin (10 μM) and DEX treatment significantly down-regulated the mRNA levels of these genes. Western blotting showed that emodin (10 μM) and DEX treatment reversed the decrease in protein expression levels of ACAN and COL2A induced by TNF-α. The protein expression of IL-1β, IL-6, MMP1, MMP3, MMP13, and PTGS2 was inhibited to some

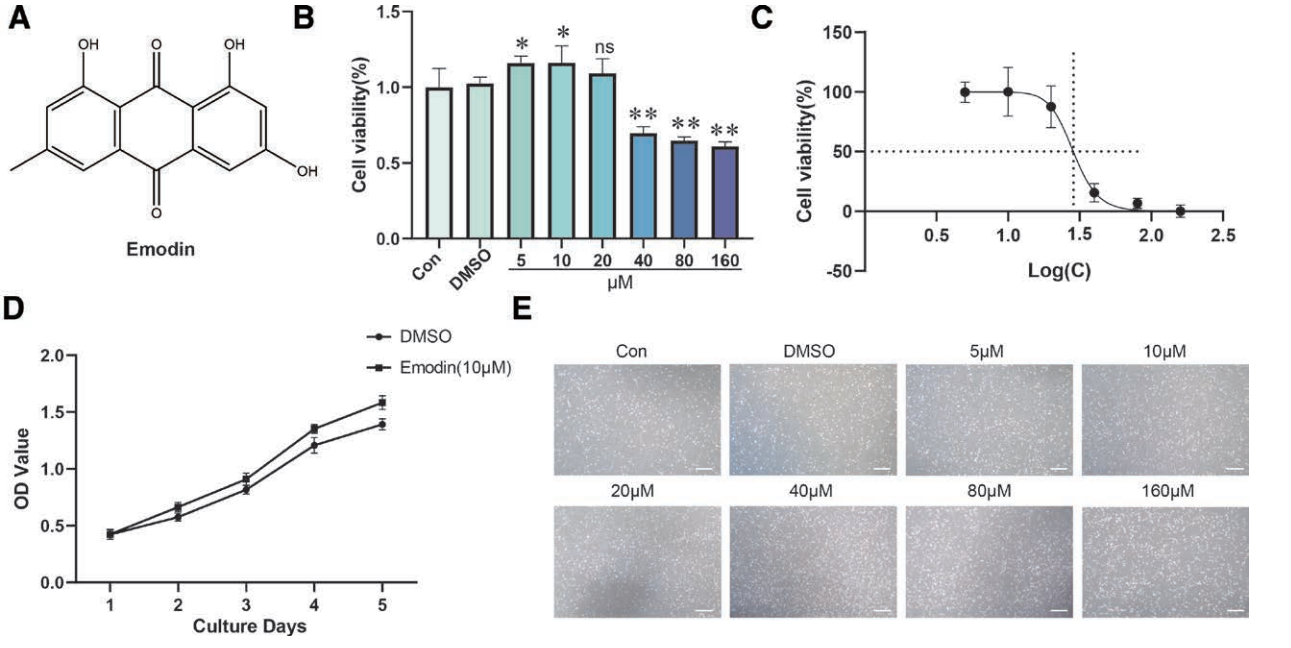

Figure 4. Cytotoxicity of emodin-treated chondrocytes. (A) Chemical structure of emodin. (B) Viability of chondrocytes treated with different concentrations of emodin for 48 h. *$P < 0.05$, **$P < 0.01$ versus the Con group. (C) IC50 values of chondrocytes treated with emodin. The horizontal coordinate represents Log(C). (D) Chondrocytes proliferation after treatment with 10 μM emodin for 5 d. (E) Images of chondrocytes treated with different concentrations of emodin for 48 h.

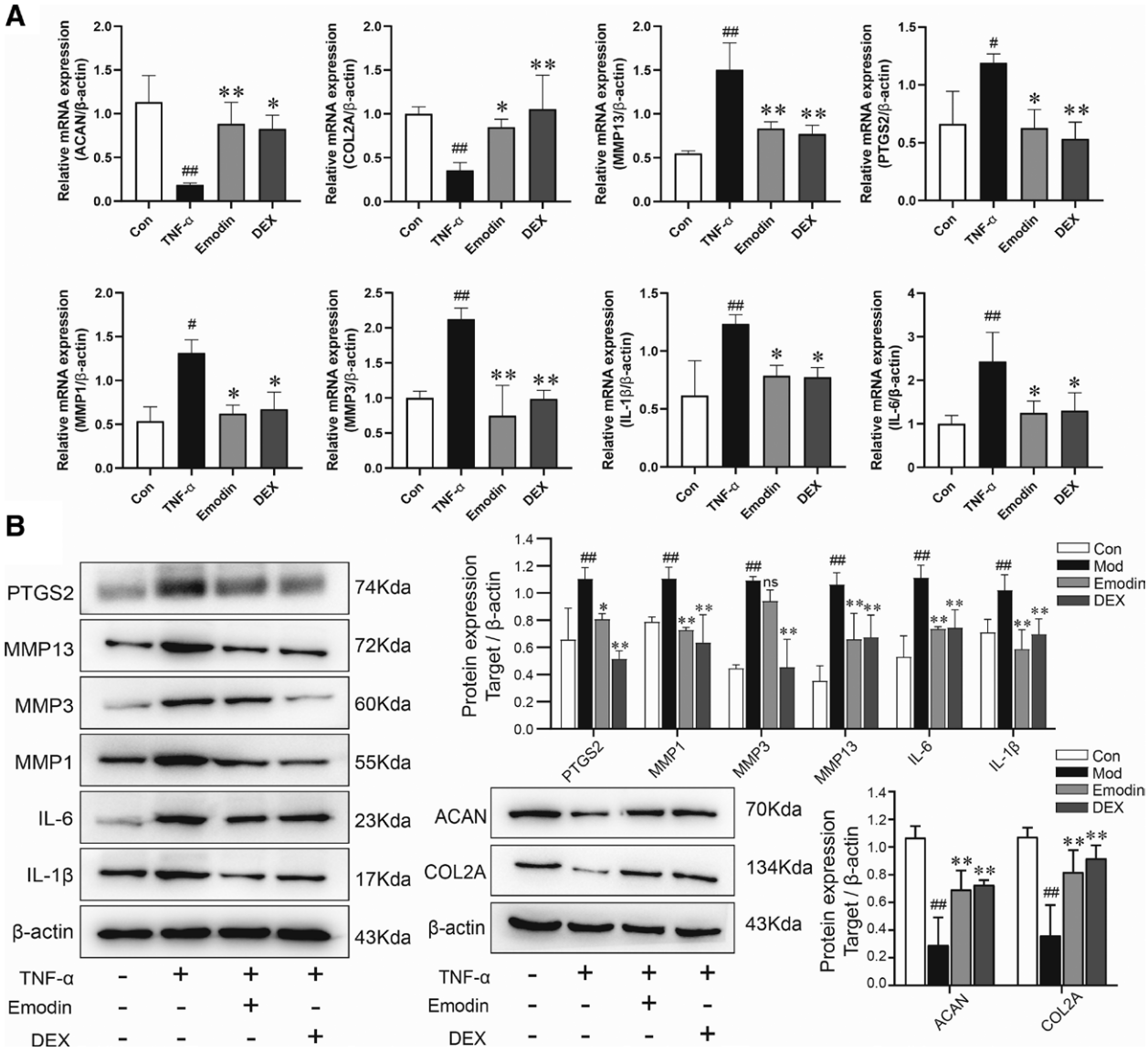

Figure 5. Emodin improves TNF-α–induced abnormal gene and protein expression. (A) The mRNA expression levels of ACAN, COL2A, IL-1β, IL-6, MMP1, MMP3, MMP13, and PTGS2 after stimulation of chondrocytes treated with TNF-α, emodin (10 μM), or DEX for 48 h. (B) Protein expression levels. $^{\#}P < 0.05$, $^{\#\#}P < 0.01$ versus the control Con group; $^{*}P < 0.05$, $^{**}P < 0.01$ versus the Mod group.

extent (Figure 5B). These results suggested that emodin has the potential to improve OA by activating cartilage matrix synthesis and inhibiting the expression of inflammatory genes.

GEO database search and pathway enrichment analysis

We downloaded a gene expression dataset generated by RNA sequencing (RNA-Seq) from the Gene Expression Omnibus (GEO, http://www.ncbi.nlm.nih.gov/geo/) under GEO accession number GSE114007. The dataset comprised 38 independent samples (18 normal and 20 arthritic cartilage tissues). We re-analyzed the data using Limma in the R language and identified 3,874 differentially expressed genes (DEGs; adj$P$ < 0.05) (Figure 6A). We then performed GO functional annotation (Figure 6B) of DEGs using the "Wu Kong" platform (https://www.omicsolution.com/wkomics/main/). In addition, KEGG enrichment analysis showed that OA was highly enriched in metabolic processes as well as the PI3K-Akt signaling pathway, MAPK signaling pathway, and other functions (Figure 6C).

Effect of emodin treatment on chondrocyte metabolism

As chondrocyte metabolic disorders are involved in the development of OA, we performed metabolomic analysis of chondrocytes after treatment with emodin by GC-MS identification of the differential metabolites between the control Con, Mod, and emodin-treated groups (Figure 7A, B). Principal component analysis (PCA) showed close clustering of metabolites between the Con and TNF-α-induced chondrocyte Mod groups (Figure 7C), indicating significant metabolic differences. Non-significant variables were excluded using OPLS-DA analysis. Only statistically significant signals were assessed. The Con group differed significantly from the TNF-α-induced chondrocyte Mod group (Figure 7D). As shown in Figure 7E, TNF-α treatment affected the production of several metabolites in the chondrocytes. In addition, 200 external experiments were

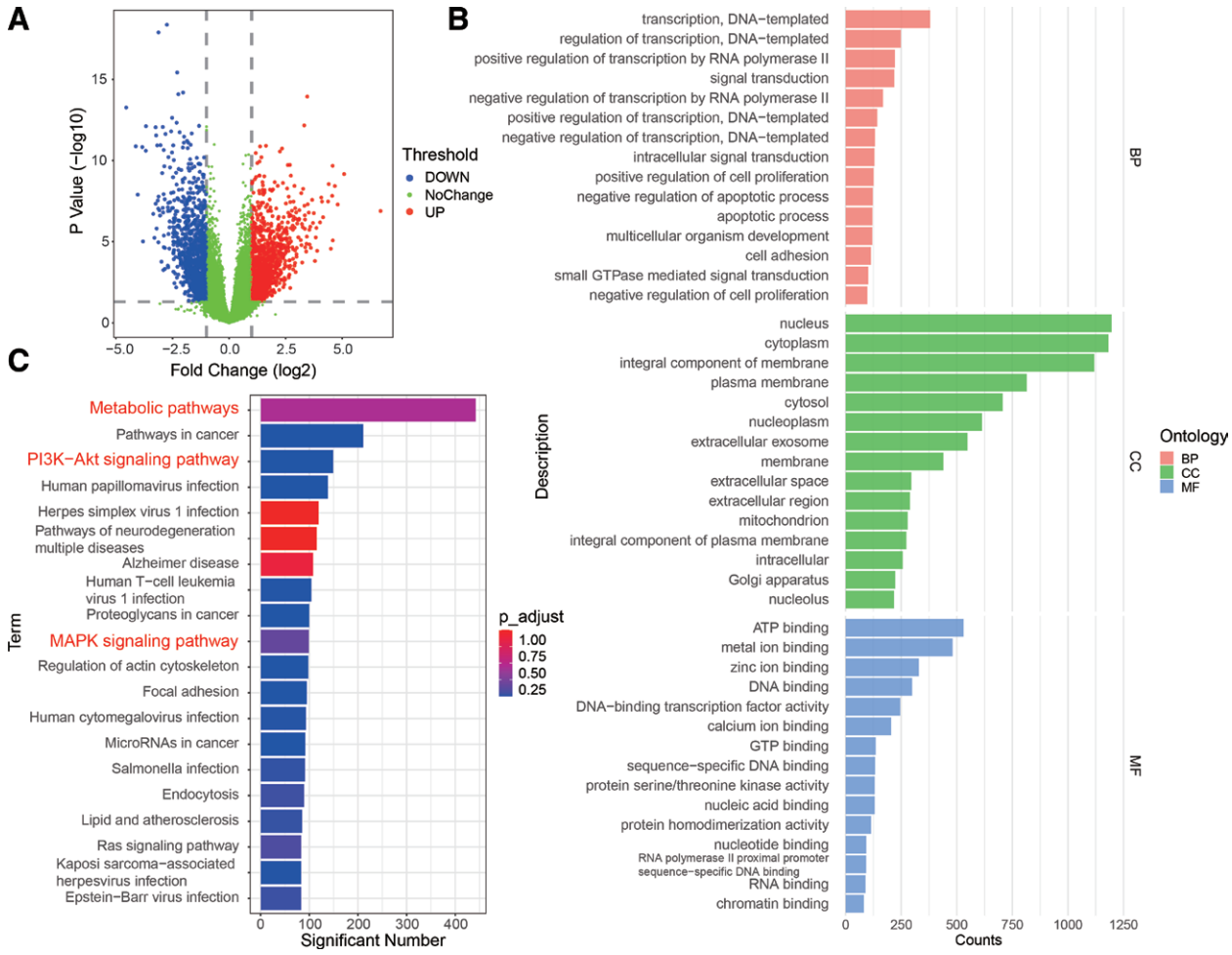

Figure 6. GEO database analysis of differential gene expression between the normal and OA groups. (A) Volcano plot of DEGs between the normal and OA groups (984 genes up-regulated; 962 genes down-regulated; fold change > 1). (B) GO functional enrichment analysis of DEGs (GO-BP, GO-CC, GO-MF). (C) KEGG enrichment analysis of DEGs. DEGs: Differentially expressed genes; GEO: Gene Expression Omnibus.

used to avoid overfitting and demonstrate the good predictive performance of our OPLS-DA model (Figure 7F). Finally, using $P < 0.05$ and VIP > 1 as selection conditions, statistical analysis showed that TNF-α treatment of chondrocytes affected the metabolic pathways, such as primary bile acid biosynthesis, steroid biosynthesis, and biosynthesis of unsaturated fatty acids. (Figure 7G). The main differential metabolites regulated by emodin included stearic acid and cholesterol (Figure 7H). These results suggest that emodin can improve OA by regulating metabolic pathways.

Molecular docking simulation of emodin with targets related to cholesterol metabolism

Cholesterol metabolism plays an important role in OA development. We performed KEGG analysis of cholesterol metabolic pathway-related regulatory proteins and constructed a PPI network diagram (Figure 8A). The top 10 proteins were listed according to their associated enrichment scores (darker red indicates higher enrichment). The degree of binding of emodin to the related proteins was demonstrated by molecular docking simulations (in which APOB could not be docked successfully and was discarded). The five molecular docking schematics shown in Figure 8B–8F revealed that emodin binds stably to APOE, ABCA1, LDLR, APOA1, and SCARB1, with combined free energy values of 7.8, 8.5, 8.7, 8.5, and 6.2 kcal/mol, respectively. These results confirm that emodin can improve the occurrence and development of OA by affecting cholesterol metabolism.

Discussion

OA is a chronic disease caused by progressive cartilage destruction combined with an inflammatory response[24]. Therefore, suppression of the inflammatory response and protection of cartilage tissue represent promising strategies to slow the progression of OA. However, no drugs can cure OA. In recent years, there has been a significant breakthrough in the treatment of OA using natural products that reduce the production of inflammatory factors and regulate chondrocyte proliferation and apoptosis[25–26].

PMT, a CMH used by clinicians has shown therapeutic effects in osteoporosis[27]. Under the guidance of Chinese medicine theory, the black bean juice stewing method can enhance its tonic effect and strengthen muscles and bones[28]. In the present study, macroscopic and microscopic evaluation of rat knee joints showed that the water extract of PMT attenuated cartilage damage and inhibited the development of OA.

Modern studies have shown that emodin is the main component of PMT[29]. The results of our HPLC analysis showed that the Z group had the highest increase in emodin content compared with the S group. In addition, according to multiple LC-MS studies, emodin and its derivatives were detected in the plasma of rats with orally administered PMT extracts[30–31], indicating that emodin can enter the blood and reach all parts of the body *via* circulation. Emodin has anti-inflammatory and analgesic effects and protects the joints. Accumulating evidence also shows that emodin has good anti-inflammatory effects[18–32], significantly inhibiting IL-1β–induced inflammatory responses in chondrocytes of patients with OA[33–34]. We showed that the proliferation of chondrocytes increased slightly after treatment with 10 μM emodin, while 40 μM emodin had a significant inhibitory effect on chondrocyte proliferation. Additionally, RT-qPCR and Western blotting showed that emodin reversed the degree of inflammation in TNF-α–treated chondrocytes and reduced cartilage matrix degradation. These results suggest that emodin exerts a protective effect on chondrocytes.

Metabolic disorders play a crucial role in the development of diseases and improving the metabolic

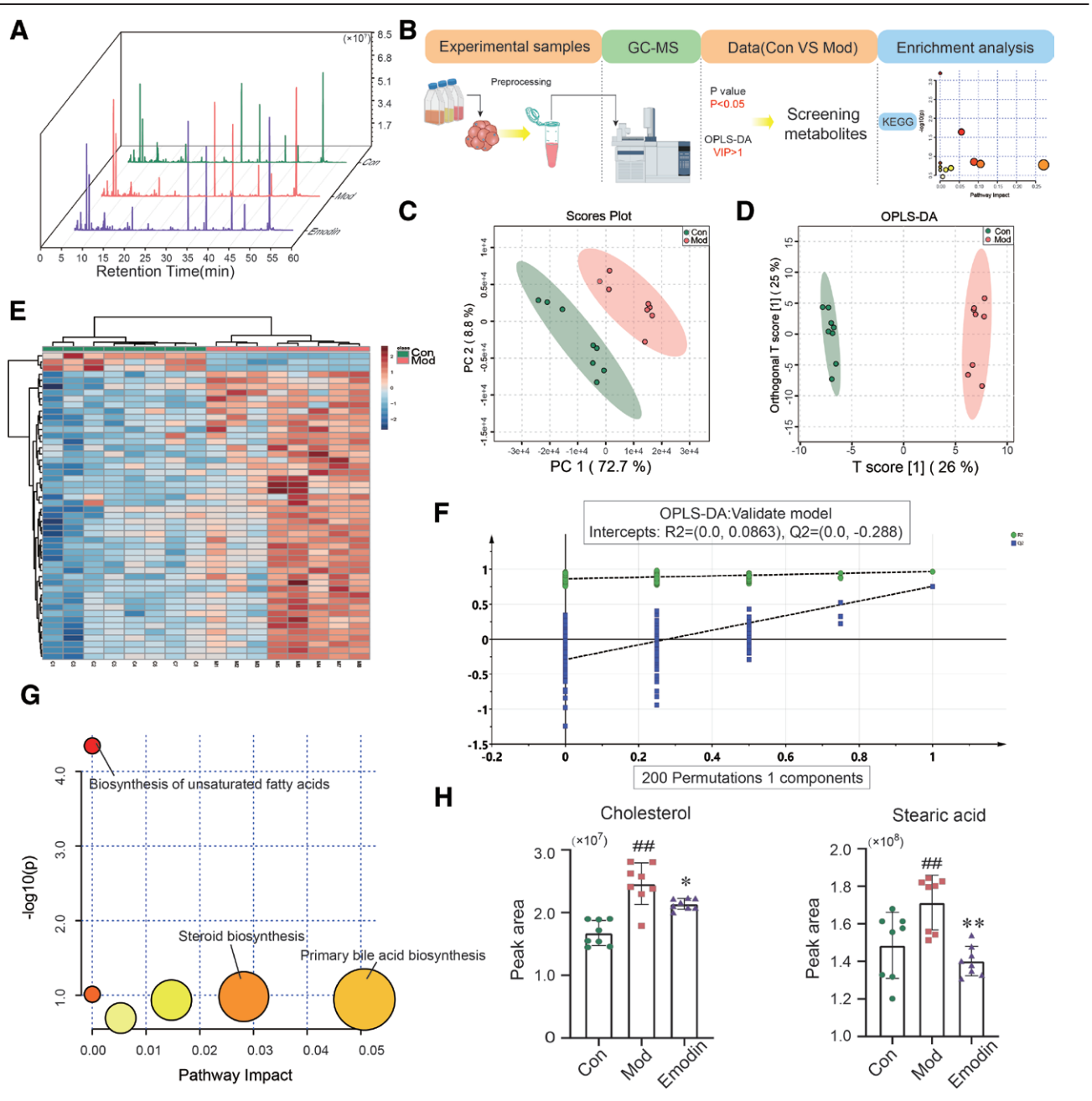

Figure 7. Emodin improves OA by regulating metabolic pathways. (A) GC-MS chromatograms of metabolites from the Con, Mod and emodin (10 μM) treatment groups. (B) Flow chart of chondrocyte sample pre-processing and data processing. (C) PCA analysis of the Con and Mod groups. (D) OPLS-DA analysis of metabolites in the Con and Mod groups. (E) Heat map of metabolites in the Con versus Mod groups. (F) 200 external validations of the OPLS-DA model. (G) Emodin-regulated metabolites for KEGG pathway analysis. (H) Statistical analysis of emodin-modulated metabolites between groups (n = 8 replicates per group). All data were analyzed using unpaired t-tests and expressed as mean ± SD. $^{\#}P < 0.05$, $^{\#\#}P < 0.01$ versus the control Con group; $^{*}P < 0.05$, $^{**}P < 0.01$ versus the Mod group. GC-MS: Gas chromatography-mass spectrometry; OA: Osteoarthritis; PCA: Principal component analysis.

environment can be beneficial for disease treatment. Lipid and glucose metabolism disorders have been reported to play key roles in the development of OA[35]. In our study, enrichment analysis of the GEO dataset showed that OA was highly correlated with metabolism. We used GC-MS metabolomic analysis to investigate the ability of emodin to improve the metabolic environment for OA treatment. Differential metabolite analysis revealed that total cholesterol and stearic acid were significantly increased in TNF-α–treated chondrocytes, whereas their levels were significantly decreased after emodin treatment[36]. We hypothesized that total cholesterol is the most important metabolite in the development of OA as previous studies have also shown that total cholesterol was significantly increased in IL-1β– or TNF-α–treated primary chondrocytes[37]. In this study, we showed that the CH25H-CYP7B1-RORα axis of cholesterol metabolism is an important catabolic regulator of OA pathogenesis. However, it is unclear whether emodin improves the metabolic environment for OA treatment through this axis. Studies have reported that primary bile acid biosynthesis is the main catabolic pathway associated with cholesterol metabolism[38]. Therefore, we performed a molecular docking simulation of cholesterol metabolism-related proteins and emodin and showed that emodin binds stably to the top 10 proteins. This suggests that APOE, ABCA1, and other targets may be potential targets of emodin in the treatment of OA through cholesterol metabolism. Therefore, we speculate that the increase in emodin content after PMT processing facilitates entry into the blood, thereby improving its ability to treat OA by regulating cholesterol metabolism and further reflecting the effect of PMT concoction on "strengthening tendons and bones."

In the present study, we demonstrated for the first time the therapeutic effect of the aqueous extract of PMT after concoction on OA, and revealed that the incremental component emodin could improve OA by regulating cholesterol metabolism. Our results suggest that the water extract after PMT concoction may exert anti-inflammatory effects by modulating potential targets, such as APOE, ABCA1, LDLR, APOA1, SCARB1, and related signaling pathways, such as inflammatory and metabolic pathways. In addition, glucose metabolism plays a crucial role in the development of OA, and we will investigate the effects of glucose metabolism on OA in the future. However, to overcome the limitations of this study, we will validate stable molecular docking targets and further investigate the molecular mechanism by which PMT consumption is associated with the incremental component emodin in the treatment of OA.

Conflict of interest statement

The authors declare no conflict of interest.

Funding

This work was supported by Hubei Provincial Central Government Guided Local Science and Technology Development Special Project "Traditional Chinese Herbal Medicine Properties and Quality Evaluation Platform" (2020ZYYD030). Hubei Province Health and Family Planning Scientific Research Project (WJ2023Q016).

Author contributions

Lanqing Li and Kang Xu designed the study. Lanqing Li, Maryam Nisar and Muhammad Farrukh Nisar performed experiments. Li and Haiying Xu analyzed and visualized

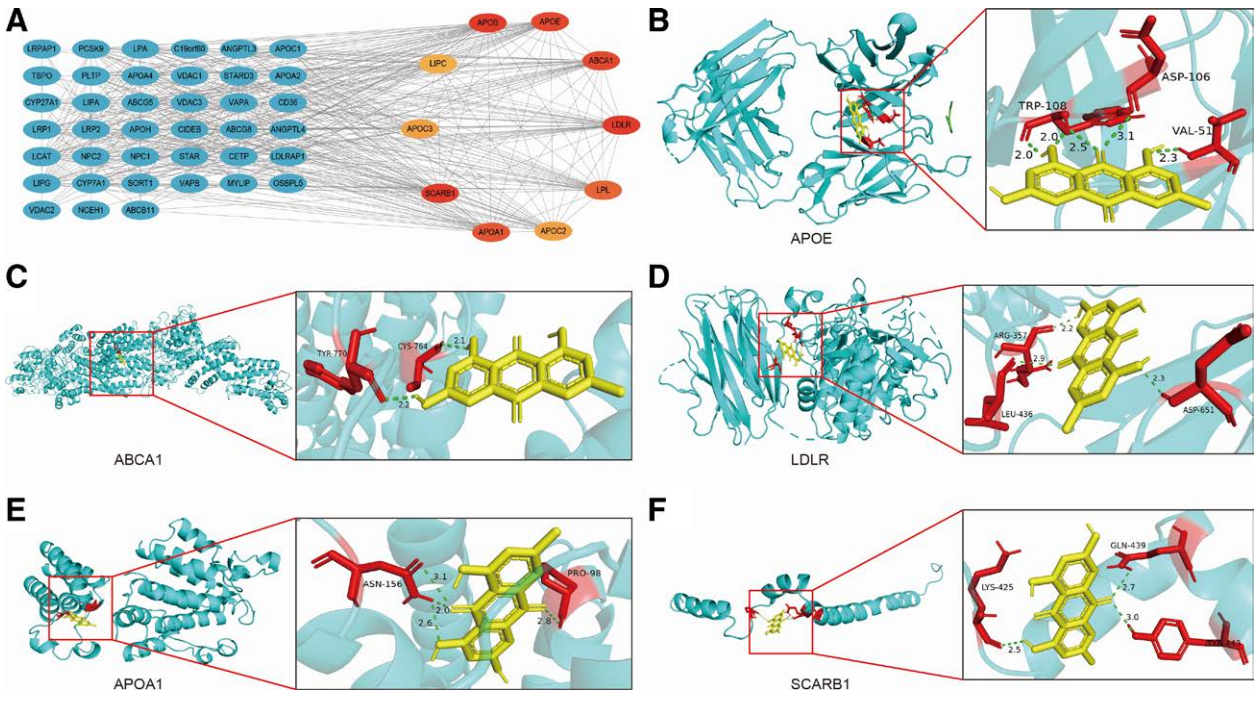

Figure 8. Molecular docking simulation showing that emodin binds stably to targets related to cholesterol metabolism. (A) PPI network diagram analysis of enzymes related to cholesterol metabolism. (B–F) Schematic diagram of molecular docking of emodin with APOE, ABCA1, LDLR, APOA1, SCARB1 proteins.

the data. Liu and Kang Xu provided research materials. Linghang Qu, Xianqiong Liu, and Kang Xu participated in compiling and revising the manuscript. All authors have proofread and approved the final version of the manuscript.

Ethical approval of studies and informed consent

All animal studies followed relevant national legislation and were approved by the Animal Care Committee of the Hubei University of Chinese Medicine (20220315007).

Acknowledgments

None.

References

[1] Wang C, Gao Y, Zhang Z, et al. Safflower yellow alleviates osteoarthritis and prevents inflammation by inhibiting PGE2 release and regulating NF-κB/SIRT1/AMPK signaling pathways. *Phytomedicine* 2020;78:153305.
[2] Hunter DJ, Bierma-Zeinstra S. Osteoarthritis. *Lancet* 2019;393(10182):1745–1759.
[3] Sacitharan PK. Ageing and Osteoarthritis. *Subcell Biochem* 2019;91:123–159.
[4] Sewell J, Östör A. Emerging injectable therapies for osteoarthritis. *Expert Opin Emerg Drugs* 2022;1:10.
[5] Cooper C. Global, regional, and national incidence, prevalence, and years lived with disability for 301 acute and chronic diseases and injuries in 188 countries, 1990-2013: a systematic analysis for the Global Burden of Disease Study 2013. *Lancet* 2015;386(9995):743–800.
[6] Bannuru RR, Osani MC, Vaysbrot EE, et al. OARSI guidelines for the non-surgical management of knee, hip, and polyarticular osteoarthritis. *Osteoarthritis Cartilage* 2019;27(11):1578–1589.
[7] Deyle GD, Allen CS, Allison SC, et al. Physical therapy versus glucocorticoid injection for osteoarthritis of the knee. *N Engl J Med* 2020;382(15):1420–1429.
[8] Kolasinski SL, Neogi T, Hochberg MC, et al. 2019 American College of rheumatology/arthritis foundation guideline for the management of osteoarthritis of the hand, hip, and knee. *Arthritis Care Res* 2020;72(2):149–162.
[9] Katz JN, Arant KR, Loeser RF. Diagnosis and treatment of hip and knee osteoarthritis: a review. *JAMA* 2021;325(6):568–578.
[10] Li F, Zhang T, He Y, et al. Inflammation inhibition and gut microbiota regulation by TSG to combat atherosclerosis in ApoE$^{(-/-)}$ mice. *J Ethnopharmacol* 2020;247:112232.
[11] Laiguillon MC, Courties A, Houard X, et al. Characterization of diabetic osteoarthritic cartilage and role of high glucose environment on chondrocyte activation: toward pathophysiological delineation of diabetes mellitus-related osteoarthritis. *Osteoarthritis Cartilage* 2015;23(9):1513–1522.
[12] Kumm J, Tamm A, Lintrop M, et al. Diagnostic and prognostic value of bone biomarkers in progressive knee osteoarthritis: a 6-year follow-up study in middle-aged subjects. *Osteoarthritis Cartilage* 2013;21(6):815–822.
[13] Huang C, Wang Y, Wang J, et al. TSG (2,3,4',5-tetrahydroxystilbene 2-O-β-D-glucoside) suppresses induction of pro-inflammatory factors by attenuating the binding activity of nuclear factor-κB in microglia. *J Neuroinflammation* 2013;10:129.
[14] Zhang JK, Yang L, Meng GL, et al. Protective effect of tetrahydroxystilbene glucoside against hydrogen peroxide-induced dysfunction and oxidative stress in osteoblastic MC3T3-E1 cells. *Eur J Pharmacol* 2012;689(1-3):31–37.
[15] Zhang W, Wang GM. The preventive effect of SWYSD on the osteoarthritis in rabbits animal model and its possible mechanism. *China Med Eng* 2011;19(6):52–3.
[16] Wang JM, Li JY, Cai H, et al. Nrf2 participates in mechanisms for reducing the toxicity and enhancing the antitumour effect of Radix Tripterygium wilfordii to S180-bearing mice by herbal-processing technology. *Pharm Biol* 2019;57(1):437–448.
[17] Xu K, Zhou T, Huang Y, et al. Anthraquinone emodin inhibits tumor necrosis factor alpha-induced calcification of human aortic valve interstitial cells via the NF-κB pathway. *Front Pharmacol* 2018;9:1328.
[18] Hwang JK, Noh EM, Moon SJ, et al. Emodin suppresses inflammatory responses and joint destruction in collagen-induced arthritic mice. *Rheumatology* 2013;52(9):1583–1591.
[19] Li L, Xu H, Qu L, et al. Daidzin inhibits hepatocellular carcinoma survival by interfering with the glycolytic/gluconeogenic pathway through downregulation of TPI1. *BioFactors* 2022;48(4):883–896.
[20] Feng F, Pan L, Wu J, et al. Cepharanthine inhibits hepatocellular carcinoma cell growth and proliferation by regulating amino acid metabolism and suppresses tumorigenesis *in vivo*. *Int J Biol Sci* 2021;17(15):4340–4352.
[21] Pan L, Feng F, Wu J, et al. Demethylzeylasteral targets lactate by inhibiting histone lactylation to suppress the tumorigenicity of liver cancer stem cells. *Pharmacol Res* 2022;181:106270.
[22] Wang C, Al-Ani MK, Sha Y, et al. Psoralen protects chondrocytes, exhibits anti-inflammatory effects on synoviocytes, and attenuates monosodium iodoacetate-induced osteoarthritis. *Int J Biol Sci* 2019;15(1):229–238.
[23] Mankin HJ, Dorfman H, Lippiello L, et al. Biochemical and metabolic abnormalities in articular cartilage from osteo-arthritic human hips. II. Correlation of morphology with biochemical and metabolic data. *J Bone Joint Surg Am* 1971;53(3):523–537.
[24] Xu K, Gao Y, Yang L, et al. Magnolin exhibits anti-inflammatory effects on chondrocytes via the NF-κB pathway for attenuating anterior cruciate ligament transection-induced osteoarthritis. *Connect Tissue Res* 2021;62(4):475–484.
[25] Gao M, Chen C, Zhang Q, et al. Research progress on the antiosteoarthritic mechanism of action of natural products. *Evid-Based Complementary Altern Med* 2021;2021:7714533.
[26] Deligiannidou GE, Papadopoulos RE, Kontogiorgis C, et al. Unraveling natural products' role in osteoarthritis management-an overview. *Antioxidants* 2020;9(4):348.
[27] Hwang YH, Kang KY, Kim JJ, et al. Effects of hot water extracts from polygonum multiflorum on ovariectomy induced osteopenia in mice. *Evid-Based Complementary Altern Med* 2016;2016:8970585.
[28] Zhu LL, Fan LD, Hu MH, et al. Hematopoietic effect of small molecular fraction of Polygoni multiflori Radix Praeparata in cyclophosphamide-induced anemia mice. *Chin J Nat Med* 2019;17(7):535–544.
[29] Shen XJ, Zhang GJ, Lv Q, et al. Advances in chemical constituents and pharmacological activities of pleuropterus multiflorus. *J Trop Subtrop Bot* 2021;29(4):439–450.
[30] Lin L, Lin H, Yin X, et al. Characterization of the constituents in rat plasma after oral administration of radix polygoni multiflori extracts by ultra-performance liquid chromatography/quadrupole time-of-flight mass spectrometry. *Biomed Chromatogr* 2015;29(10):1541–1547.
[31] Zhang J, Wang T, Ren Z, et al. Application of HPLC-LTQ Orbitrap MS for metabolic profiles of Polygonum multiflora extract in rats. *Biomed Chromatogr* 2018;32(2):e4067.
[32] Zhu X, Zeng K, Qiu Y, et al. Therapeutic effect of emodin on collagen-induced arthritis in mice. *Inflammation* 2013;36(6):1253–1259.
[33] Hu H, Song X, Li Y, et al. Emodin protects knee joint cartilage in rats through anti-matrix degradation pathway: an in vitro and in vivo study. *Life Sci* 2021;269:119001.
[34] Ding QH, Ye CY, Chen EM, et al. Emodin ameliorates cartilage degradation in osteoarthritis by inhibiting NF-κB and Wnt/β-catenin signaling in vitro and in vivo. *Int Immunopharmacol* 2018;61:222–230.
[35] Clockaerts S, Van Osch GJ, Bastiaansen-Jenniskens YM, et al. Statin use is associated with reduced incidence and progression of knee osteoarthritis in the Rotterdam study. *Ann Rheum Dis* 2012;71(5):642–647.
[36] Sekar S, Shafie SR, Prasadam I, et al. Saturated fatty acids induce development of both metabolic syndrome and osteoarthritis in rats. *Sci Rep* 2017;7:46457.
[37] Choi WS, Lee G, Song WH, et al. The CH25H-CYP7B1-RORα axis of cholesterol metabolism regulates osteoarthritis. *Nature* 2019;566(7743):254–258.
[38] Yu Z, Shi Z, Zheng Z, et al. DEHP induce cholesterol imbalance via disturbing bile acid metabolism by altering the composition of gut microbiota in rats. *Chemosphere* 2021;263:127959.

How to cite this article: Li LQ, Xu HY, Qu LH, Maryam N, Muhammad FN, Liu XQ, Xu K. Water extracts of *Polygonum Multiflorum Thunb.* and its active component emodin relieves osteoarthritis by regulating cholesterol metabolism and suppressing chondrocyte inflammation. Acupunct Herb Med 2023;3(2):96–106. doi: 10.1097/HM9.0000000000000061